2019 American Control Conference (ACC)
Philadelphia, PA, USA, July 10-12, 2019

Parameter Estimation in Type 1 Diabetes Models for Model-Based Control Applications

Dimitri Boiroux, Zeinab Mahmoudi, John Bagterp Jørgensen

Abstract— **In this paper, we discuss the identification of a physiological model describing the glucose-insulin dynamics in people with type 1 diabetes (T1D). The identified model has to be applied to nonlinear model predictive control (NMPC). We propose a stochastic model of the glucose-insulin dynamics in T1D. Discrete-time glucose data are provided by a continuous glucose monitor (CGM). We use maximum likelihood for parameter estimation, combined with a procedure to compute the gradient of the likelihood function. To test our identification procedure, we generate a virtual population of 10 patients using the Hovorka model and its parameter distribution. We report the estimates of the model parameters, and we use a validation dataset to evaluate the prediction errors for different prediction intervals. Whereas short-term predictions of blood glucose concentrations are consistent among patients, the accuracy of long-term predictions is more subject to inter-patient variability. The results suggest that this method has the potential to be used in NMPC algorithms.**

I. Introduction

White-box models are usually derived from first order principles. They are able to capture the nonlinear dynamics of a given system but cannot easily accommodate process noise. Conversely, black-box models are data-driven. They allow to quantify the process noise, but the physical meaning of the different states is lost. Grey-box models using stochastic differential equations (SDEs) attempt to combine the advantages of white- and black-box modeling [1]. Grey-box models keep the physical relevance of the model parameters while being able to incorporate and quantify process noise.

In type 1 diabetes (T1D), the effect of administered insulin and the blood glucose concentration are affected by a number of factors, such as carbohydrates from meals, stress, illness or physical activity. These factors are difficult to quantify through direct observations. Manual carbohydrate counting remains a challenge for most people with T1D [2]. The effects of physical activity on blood glucose concentration are still not completely elucidated [3]. To quantify the effect of the aforementioned factors, modeling based on continuous-discrete stochastic differential equations (SDEs) applied to T1D have shown promising results [4]–[6]. In the work from Duun-Henriksen and colleagues [4], interstitial glucose measurements from continuous glucose monitors (CGMs) and blood glucose measurements from a YSI (Yellow Spring Instruments) have been used to identified a stochastic model. Visentin and colleagues used maximum a posteriori (MAP) to identify the model used in the UVa/Padova simulator [7]. Haidar and colleagues used an approach based on Markov chain Monte Carlo [8]. In practice, patients only have access to glucose measurements from a CGM. In the work from [5], the stochastic model has been identified using overnight CGM measurements only and does not include the nonlinear prandial dynamics. In our previous work [6], we showed the identification of a physiological model for T1D using CGM data, but some parameters were highly uncertain, suggesting that our model was overparametrized.

Reliable T1D models able to predict blood glucose concentrations are crucial for the development of an artificial pancreas (AP). The AP refers to automated administration of drugs for the treatment of type 1 diabetes [9]–[11]. Current AP prototypes comprise a CGM, a control algorithm implemented on a mobile platform and an insulin pump. The estimator computes the state estimates and predictions through an continuous-discrete extended Kalman filter (CDEKF) and identifies the parameters of the T1D model using maximum likelihood. The detector detects faulty CGM measurements, eg. drifts, as well as meal time and size by using a specific algorithm for meal estimation [12]–[15]. The MPC algorithm uses the model and states provided by the Kalman filter and meal information to predict and optimize future insulin injections. Smart bolus calculators may be used to compute prandial insulin boluses [16]–[19]. The insulin pump implements the suggested basal and/or boluses subcutaneously. Fig. 1 illustrates the AP.

Model predictive control (MPC) is a model-based control technology. The algorithm attempts to optimize the future outcome of a given system based on past data and model predictions. In previous works, algorithms based on linear MPC were tuned using prior patient information, eg. body weight, total daily insulin, insulin sensitivity factor or insulin action time [20]–[22]. This procedure may be useful for short-term use but lacks the ability to adapt to metabolic changes in the longer run. To handle intra-patient variability, adaptive control algorithms have been developed [23], [24]. Nonlinear identifiable models usable in an AP could handle metabolic variations and more complex dynamics, but the tuning and the adaptation of control algorithms based on nonlinear models for the AP remains a tedious process.

This paper focuses on the design of a nonlinear estimator for the AP. We present a nonlinear and identifiable model for T1D derived from a minimal model. This model includes the effect of subcutaneously administered insulin, the contribution from carbohydrates from meals, as well as the lag and

This work is funded by the Danish Diabetes Academy supported by the Novo Nordisk Foundation

[1]Dimitri Boiroux, Zeinab Mahmoudi and John Bagterp Jørgensen are with the Department of Applied Mathematics and Computer Science, Technical University of Denmark, DK-2800 Kgs. Lyngby, Denmark. {dibo,zeinabm,jbjo}@dtu.dk

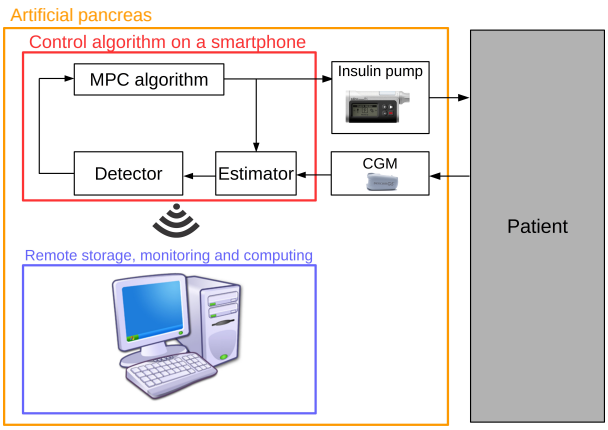

Fig. 1. Diagram of the artificial pancreas. The estimator uses a CDEKF to estimate states, parameters, and to compute the state predictions. The detector estimates the meals times and size and detects the CGM drifts based on the identified model and innovations provided by the estimator. The MPC algorithm optimizes the future insulin injections and computes the state predictions.

noise from CGMs. The model also incorporates a stochastic part to quantify the different unknown factors affecting blood glucose concentrations. We identify the parameters for prediction using maximum likelihood with a continuous-discrete EKF. We test the identifiability of this model and we numerically evaluate the ability of the identified model to predict future blood glucose concentrations on a cohort of 10 virtual patients generated using a different model.

This paper is structured as follows. Section II describes the modified minimal stochastic model used for identification. In Section III, we present the maximum likelihood method used to identify the T1D model. In Section IV, we numerically evaluate the performance of our identification method and we assess the accuracy of glucose concentration predictions. Section V summarizes the main contributions of this paper.

II. Physiological Model of Glucose-Insulin Dynamics

In this section, we present an identifiable model describing the glucose-insulin dynamics in T1D. This model is derived from the Medtronic Virtual Patient (MVP) model [25]. Fig. 2 illustrates the MVP model. We add the CGM noise model developed by [26] to represent (i) the glucose transport from blood glucose, $G(t)$, to interstitial tissues, $G_I(t)$, and (ii) the sensor noise. We formulate this model as a continuous-discrete stochastic differential equation model in the form

$$dx(t) = f(t, x(t), u(t), d(t), \theta)dt + \sigma(\theta)dw(t), \quad (1a)$$
$$y_k = g(x_k) + v_k. \quad (1b)$$

The SDE model (1a) describes the effect on subcutaneously administered insulin, $u(t)$, and the CHO absorption rate, $d(t)$, on the model states, $x(t)$. We assume that $w(t) \sim N_{iid}(0, Idt)$ is a standard Wiener process. The measurements, y_k, are taken at discrete times. $g(x_k)$ is the sensor

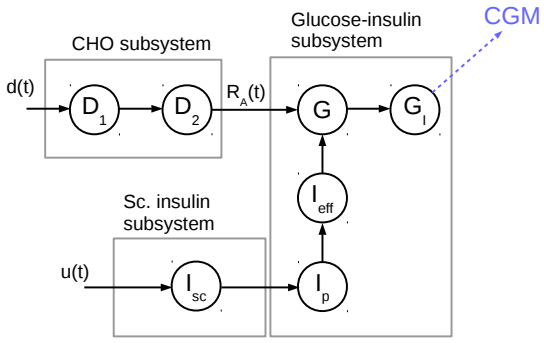

Fig. 2. The MVP model. This model simulates the action of subcutaneously administered insulin on BG concentration, the effects of meals, interstitial glucose and CGM measurements.

function and $v_k \sim N_{iid}(0, R(\theta))$ represents the sensor noise. The diffusion term, $\sigma(\theta)$, quantifies the process noise in continuous time.

A. Insulin Absorption Subsystem

The insulin absorption subsystem models the subcutaneous insulin concentration, $I_{SC}(t)$ [mU/L/min], and the plasma insulin concentration, $I_P(t)$ [mU/L]. It is described by the two-compartment model

$$dI_{SC} = k_1 \left(\frac{u(t)}{C_I} - I_{SC}(t) \right) dt + \sigma_1 d\omega_1, \quad (2a)$$
$$dI_P = k_2 \left(I_{SC}(t) - I_P(t) \right) dt + \sigma_2 d\omega_2, \quad (2b)$$

where $u(t)$ [mU/min] is the insulin infusion rate and C_I [L/min] is the clearance rate. k_1 and k_2 [min^{-1}] are the inverses of time constants associated to insulin absorption.

B. Insulin-Glucose Dynamics

The effect of insulin, $I_{EFF}(t)$ [min^{-1}], and the blood glucose concentration, $G(t)$ [mg/dL], are described by the following SDEs

$$dI_{EFF} = \left(-p_2 I_{EFF}(t) + p_2 S_I I_P(t) \right) dt + \sigma_3 d\omega_3, \quad (2c)$$
$$dG = \left(-(I_{EFF}(t) + GEZI) G(t) + EGP + R_A(t) \right) dt + \sigma_4 d\omega_4, \quad (2d)$$

in which S_I [mL/mU] is the insulin sensitivity, p_2 [min^{-1}] is the inverse of a time constant, $GEZI$ [min^{-1}] is the glucose effectiveness at zero insulin, EGP [mg/dL/min] is the endogenous glucose production, and $R_A(t)$ [mg/dL/min] is the rate of appearance contribution from the meals.

C. CHO Absorption Model

The two-compartment model introduced by [27] describes the CHO absorption and conversion to glucose. It is

$$dD_1 = \left(d(t) - \frac{D_1(t)}{\tau_G} \right) dt + \sigma_5 d\omega_5, \quad (2e)$$
$$dD_2 = \left(\frac{D_1(t) - D_2(t)}{\tau_G} \right) dt + \sigma_6 d\omega_6, \quad (2f)$$
$$R_A(t) = \frac{D_2(t) k_m}{V_G}. \quad (2g)$$

$d(t)$ [mg/min] is the CHO intake. k_m [min] is the inverse of the meal absorption time constant and V_G [dL] is the glucose distribution volume.

D. Identifiable model

Even the simplest nonlinear models for T1D may be difficult to identify ([28]). In particular, the terms related to time constants, k_1, k_2 and p_2, as well as the glucose effectiveness at zero insulin, $GEZI$, are highly uncertain. Therefore, based on our previous work and these observations, we suggest the following simplifications: (i) We use only one term to describe the inverse of the time constants, k_1, k_2 and p_2, (ii) we fix the insulin clearance rate, C_I, because it cannot be distinguished from the insulin sensitivity when only CGM measurements are available, (iii) we set $GEZI = 0$ and (iv) we only identify the diffusion term related to blood glucose concentration, σ_4.

III. Maximum likelihood estimation

In this section, we describe the maximum likelihood estimation procedure. Given a sequence of observations

$$\mathcal{Y}_N = \{y_0, y_1, \dots, y_N\}, \tag{3}$$

we want to maximize the joint probability density

$$p(\mathcal{Y}_N|\theta) = p(y_N, y_{N-1}, \cdots, y_0|\theta), \tag{4}$$

i.e. to maximize the likelihood function. Maximizing the likelihood function, or equivalently minimizing the -log-likelihood function, provides an estimate of the parameters θ in (1).

A. Continuous-discrete extended Kalman filter

We recall here the CDEKF for nonlinear continuous-discrete stochastic nonlinear systems ([29], [30]). The filtering in the CDEKF describes the steps used to compute the filtered state, $\hat{x}_{k|k}$, and the corresponding covariance, $P_{k|k}$. The prediction step computes the mean and covariance of the one-step predictions, $\hat{x}_{k|k-1}$ and $P_{k|k-1}$.

The filter gain is computed by

$$R_{e,k} = CP_{k|k-1}C' + R, \tag{5a}$$
$$K_k = P_{k|k-1}C'R_{e,k}^{-1}. \tag{5b}$$

The innovation is the difference between the measurement, y_k, and the one-step prediction of the output, $C_k\hat{x}_{k|k-1}$. It is

$$e_k = y_k - C_k\hat{x}_{k|k-1}, \tag{6}$$

where

$$C_k = \frac{\partial g}{\partial x}(\hat{x}_{k|k-1}) \tag{7}$$

provides a linearization of the output function g evaluated at $\hat{x}_{k|k-1}$.

The filtered state, $\hat{x}_{k|k}$, and its covariance $P_{k|k}$ are given by

$$\hat{x}_{k|k} = \hat{x}_{k|k-1} + K_k e_k, \tag{8a}$$
$$P_{k|k} = P_{k|k-1} - K_k R_{e,k} K_k'. \tag{8b}$$

Remark 1 *Alternatively, one may consider the alternative expression of the state covariance matrix update [31]*

$$P_{k|k} = (I - K_kC_k)P_{k|k-1}(I - K_kC_k)' + K_kR_{e,k}K_k'. \tag{9}$$

Although (8b) *and* (9) *are mathematically equivalent, the latter guarantees the positive definiteness of $P_{k|k}$ numerically.*

The predicted state vector $\hat{x}_{k+1|k} = \hat{x}_k(t_{k+1})$ and its associated covariance $P_{k+1|k} = P_k(t_{k+1})$ are computed as the solutions to the system of ordinary differential equations ([32])

$$\frac{d\hat{x}_k(t)}{dt} = f(t, \hat{x}_k(t), u_k), \tag{10a}$$
$$\frac{dP_k(t)}{dt} = A_k(t)P_k(t) + P_k(t)A_k(t)' + \sigma\sigma', \tag{10b}$$

with

$$A_k(t) = A(t, \hat{x}_k(t), u_k) = \frac{\partial f}{\partial x}(t, \hat{x}_k(t), u_k) \tag{11}$$

given the initial conditions

$$\hat{x}_k(t_k) = \hat{x}_{k|k}, \tag{12a}$$
$$P_k(t_k) = P_{k|k}. \tag{12b}$$

B. Maximum likelihood

In the case where the sampling time is fast enough compared to the nonlinearities in (1), the first order Taylor approximation in the CDEKF (10a) still ensures that the conditional probability densities $p(Y_N|\theta)$ are normally distributed [33]. In this case, the -log-likelihood function of (1) can reasonably be approximated as [34]

$$\begin{aligned} V(\theta) &= -\ln\left(p(\mathcal{Y}_N|\theta)\right) \\ &= \frac{(N+1)n_y}{2}\ln(2\pi) + \\ &\quad \frac{1}{2}\sum_{k=0}^{N}\ln\left[\det(R_{e,k})\right] + e_k'R_{e,k}^{-1}e_k. \end{aligned} \tag{13}$$

The CDEKF computes the innovation, e_k, and its covariance, $R_{e,k}$. The model parameters estimate $\hat{\theta}$ is the minimizer of (13), i.e.

$$\hat{\theta} = \underset{\theta}{\operatorname{argmin}}\left(L(\theta)\right). \tag{14}$$

Taking the gradient of (13) with respect to the parameter vector yields

$$\begin{aligned} \frac{\partial V}{\partial \theta_i} &= \sum_{k=0}^{N}\frac{1}{2}\mathrm{tr}\left[R_{e,k}^{-1}\frac{\partial R_{e,k}}{\partial \theta_i}\right] + e_k'R_{e,k}^{-1}\frac{\partial e_k}{\partial \theta_i} \\ &\quad + \frac{1}{2}e_k'R_{e,k}^{-1}\frac{\partial R_{e,k}}{\partial \theta_i}R_{e,k}^{-1}e_k. \end{aligned} \tag{15}$$

Taking the derivatives of the Kalman filter equations allows to compute the gradient of the likelihood function (15) [35]. Instead, we use a computationally efficient implementation for maximum likelihood estimation and the computation of the likelihood function gradient (15). The computation of the likelihood function uses UD-decompositions of symmetric matrices, ie.

$$X = U_X D_X U_X', \tag{16}$$

where X is a symmetric matrix, U_X is a unit upper triangular matrix and D_X is a diagonal matrix. We use a modified weighted Gram-Schmidt decomposition to perform operation on symmetric matrices and to compute gradients, and we present a way to efficiently compute the state covariance sensitivities using a discretization of (10b) [36]. For more information about the implementation of the likelihood function computation, the reader is referred to [37].

IV. Numerical results and discussion

In this section, we illustrate the maximum likelihood estimation in a virtual population of people with T1D. The population has been randomly generated using the model and the parameter distribution from Hovorka and colleagues [22], [38], [39]. We generate a dataset based on a 30-hour scenario with a sensor sampling time of 5 minutes. In this scenario, the patient is having the following meals: a 72g CHO breakbast at 8:00, a 36g CHO snack at 11:30, a 131g CHO lunch at 13:15, a 51g CHO dinner at 18:00 and a 70g CHO snack at 22:00. The meal times and sizes are taken from [25]. At mealtime, we provide an insulin bolus. The inputs (insulin infusion rate and meal size) are assumed to be known, and a CGM provides noise-corrupted measurements in discrete time with a sampling time $T_s = 5$ minutes. We use a random insulin administration sequence and keep the insulin injection rate constant in 3-hour time windows, such that we identify the time constants of the model. We use the Euler-Maruyama method with a constant step size to solve numerically the SDEs [40]. Fig. 3 shows an example of training data for one of the 10 patients (Patient 1).

We use a validation dataset with different meal sizes (60g CHO at 6:00, 80g CHO at 12:00, 70g CHO at 18:00) and different noise realizations. We use the validation dataset to test the ability of the identified model to predict future BG concentrations.

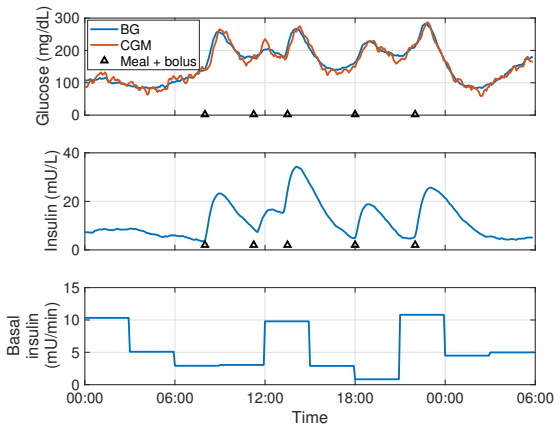

Fig. 3. Example of dataset used for identification for Patient 1. Top: BG concentration and interstitial glucose concentration measured by a CGM. Middle: Insulin concentration. Bottom: Basal insulin injections.

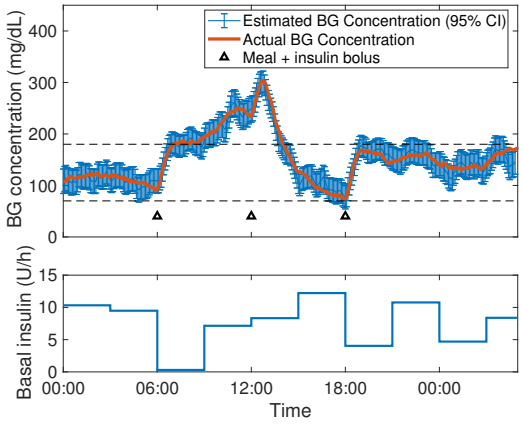

Fig. 4. Actual end estimated (with 95% confidence interval) BG concentration (top) and basal insulin injections (bottom) for Patient 1.

A. Parameter estimation

Table I shows the parameter estimates and standard deviation for the 10 considered patients. The covariance of the parameters, θ, is computed as the inverse of the Hessian, ie. ([41]

$$\mathrm{Cov}(\theta) = H^{-1}. \tag{17}$$

The standard deviation of the parameter θ_i is

$$\sigma_{\theta_i} = \sqrt{[H^{-1}]_{i,i}}. \tag{18}$$

From Table I we observe that the identified parameters are significant. However, the endogenous glucose production, EGP_0, has a higher standard deviation than the other parameters.

Table II shows the correlation matrix of the identified parameters. The correlation matrix, R, is given by

$$\Sigma_\theta = \mathrm{diag}(\sigma_\theta) \cdot R \cdot \mathrm{diag}(\sigma_\theta), \tag{19}$$

in which Σ_θ is the parameter covariance matrix. By using the results from Table I and the correlation matrix, it is possible to use the prior distribution of the parameter estimates, ie. $\theta \sim N(\theta^*, P_\theta)$. The function for a posteriori estimation is

$$V_{MAP}(\theta) = V_{ML}(\theta) + \frac{1}{2}(\theta - \theta^*)' P_\theta^{-1} (\theta - \theta^*), \tag{20}$$

in which $V_{ML}(\theta)$ is the likelihood function value (13).

B. Glucose estimation and prediction

Fig. 4 shows the actual and estimated BG concentration for a specific patient using the validation dataset, along with the 95% confidence interval on the BG concentration. We see here that despite the transport lag between the plasma and interstitial tissues, the Kalman filter is able to track the BG concentration based on CGM measurements only.

The ability to make accurate prediction of the glucose level is crucial, especially for model-based control applications. To evaluate the predictions of the model, we use our validation dataset. Fig. 5 shows the blood glucose predictions for 1 step (5 minutes), 6 steps (30 minutes), 12 steps (1 hour) and 24 steps (2 hours). To allow the comparison of the different prediction intervals under the same conditions, we

TABLE I

NUMERICAL VALUE OF THE PARAMETER ESTIMATES. THE NUMBERS SHOW THE OPTIMAL VALUE (STANDARD DEVIATION).

Patient	k_1, k_2, p_2 (min^{-1})	S_I (mL/mU/min)	EGP_0 (mg/dL/min)	$1/V_G$ (dL^{-1})	k_m (min^{-1})	σ_4 (mg/dL/min)
1	0.023 (0.0017)	0.0017 (0.0003)	1.17 (0.23)	0.0082 (0.0018)	0.0226 (0.0024)	2.91 (0.29)
2	0.015 (0.0017)	0.0011 (0.0005)	0.98 (0.38)	0.004 (0.0009)	0.022 (0.004)	3.15 (0.28)
3	0.021 (0.0017)	0.0014 (0.0004)	0.87 (0.28)	0.007 (0.0017)	0.026 (0.0038)	3.15 (0.33)
4	0.018 (0.0022)	0.0019 (0.0006)	1.47 (0.45)	0.0059 (0.0021)	0.018 (0.003)	3.07 (0.36)
5	0.012 (0.0005)	0.0024 (0.0003)	1.57 (0.23)	0.021 (0.0032)	0.015 (0.0008)	3.28 (0.32)
6	0.012 (0.0008)	0.0018 (0.0004)	1.49 (0.35)	0.0020 (0.0044)	0.014 (0.0009)	3.60 (0.38)
7	0.014 (0.0019)	0.0016 (0.0008)	1.07 (0.40)	0.013 (0.0067)	0.017 (0.0040)	3.13 (0.37)
8	0.016 (0.0016)	0.0011 (0.0002)	0.94 (0.21)	0.0036 (0.0005)	0.040 (0.0044)	3.08 (0.32)
9	0.014 (0.0019)	0.0005 (0.0001)	0.35 (0.13)	0.0044 (0.0004)	0.041 (0.0035)	2.78 (0.29)
10	0.017 (0.0021)	0.0008 (0.0002)	0.67 (0.19)	0.0039 (0.0009)	0.034 (0.0057)	3.14 (0.31)
Mean	0.017 (0.0033)	0.0013 (0.0006)	0.958 (0.39)	0.0074 (0.0056)	0.027 (0.0099)	3.05 (0.17)

TABLE II

CORRELATION MATRIX OF THE PARAMETER ESTIMATES.

	k_1	S_I	EGP_0	V_G	k_m	σ_4
k_1	1					
S_I	0.098	1				
EGP_0	0.085	0.951	1			
V_G	-0.321	0.799	0.666	1		
k_m	-0.032	-0.844	-0.833	-0.684	1	
σ_4	-0.134	0.677	0.656	0.541	-0.593	1

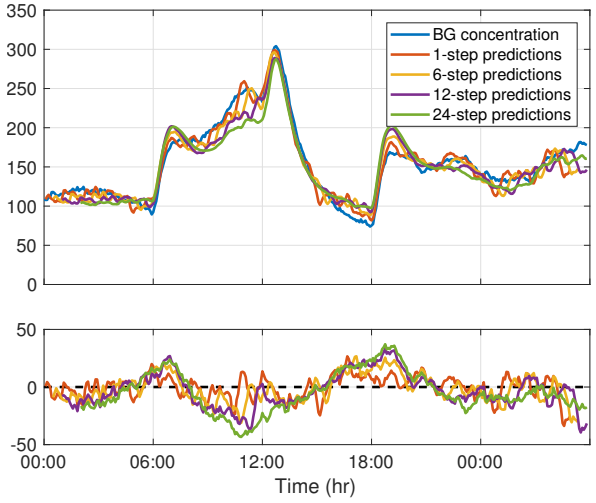

Fig. 5. BG concentration predictions (top) and prediction errors (bottom) for 1-step (5 minutes), 6-step (30 minutes), 12-step (1 hour) and 24-step (2 hours) predictions.

assume that we have perfect knowledge of the meals, which is usually not the case in reality.

The relative mean square error (RMSE) is used to evaluate the accuracy of predicted interstitial and blood glucose concentrations. The RMSE is given by

$$RMSE = \sqrt{\frac{\sum_{k=1}^{N}(\bar{y}_i - \hat{y}_i)^2}{N}}, \qquad (21)$$

in which $\hat{y}_i$ is the estimated output from the model and $\bar{y}_i$ is the actual output value.

Fig. 6 summarizes the RMSE (median, interquartile range, minimum/maximum) for the 10 patients for the different prediction interval lengths. As expected, the accuracy of

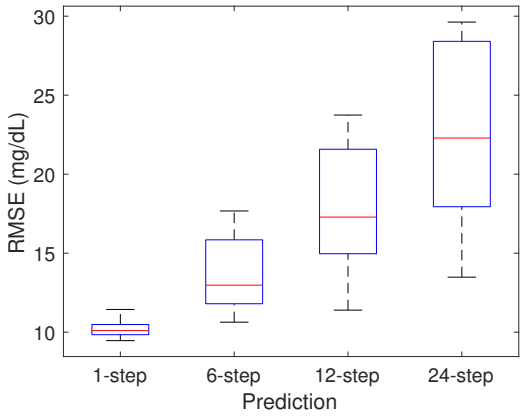

Fig. 6. Box plot of the BG concentration RMSE for different prediction intervals (median, interquartile range, minimum/maximum). The different prediction horizons are: 1 step (5 minutes), 6 steps (30 minutes), 12 steps (1 hour) and 24 steps (2 hours).

the predictions tend to deteriorate over time. For 1-step predictions, the median RMSE is approximately 11 mg/dL and the inter-patient variability is low (min. 10 mg/dL, max. 12.5 mg/dL). We also notice that the uncertainties of long-term predictions of BG concentrations are highly subject to inter-patient variability.

V. CONCLUSION

In this paper, we presented and numerically evaluated the implementation of an estimator used in the AP. The estimator uses a modified and identifiable model for T1D when only CGM measurements are available, and we demonstrated the use of maximum likelihood to estimate the parameters in this model. This model can potentially be applied to NMPC. Further simulations and test of NMPC algorithms using the identified model will be required to validate these results.

REFERENCES

[1] N. R. Kristensen, H. Madsen, and S. B. Jørgensen, "Parameter estimation in stochastic grey-box models," *Automatica*, vol. 40, pp. 225 – 237, 2004.

[2] A. Brazeau, H. Mircescu, K. Desjardins, C. Leroux, I. Strychar, J. Ekoé, and R. Rabasa-Lhoret, "Carbohydrate counting accuracy and blood glucose variability in adults with type 1 diabetes," *Diabetes Research and Clinical Practice*, vol. 99, no. 1, pp. 19–23, 2013.

[3] M. D. Breton, "Handling exercise during closed loop control," *Diabetes Technology & Therapeutics*, vol. 19, no. 6, pp. 328–330, 2017.

[4] A. K. Duun-Henriksen, S. Schmidt, R. M. Røge, J. B. Møller, K. Nørgaard, J. B. Jørgensen, and H. Madsen, "Model identification using stochastic differential equation grey-box models in diabetes," *Journal of diabetes science and technology*, vol. 7, no. 2, pp. 431–440, 2013.

[5] A. H. Hansen, A. K. Duun-Henriksen, R. Juhl, S. Schmidt, K. Nørgaard, J. B. Jørgensen, and H. Madsen, "Predicting plasma glucose from interstitial glucose observations using bayesian methods," *Journal of diabetes science and technology*, vol. 8, no. 2, pp. 321–330, 2014.

[6] D. Boiroux, M. Hagdrup, Z. Mahmoudi, N. K. Poulsen, H. Madsen, and J. B. Jørgensen, "Model identification using continuous glucose monitoring data for type 1 diabetes," *IFAC-PapersOnLine*, vol. 49, no. 7, pp. 759–764, 2016.

[7] R. Visentin, C. Dalla Man, and C. Cobelli, "One-day Bayesian cloning of type 1 diabetes subjects: toward a single-day UVA/Padova type 1 diabetes simulator," *IEEE Transactions on Biomedical Engineering*, vol. 63, no. 11, pp. 2416–2424, 2016.

[8] A. Haidar, M. E. Wilinska, J. A. Graveston, and R. Hovorka, "Stochastic virtual population of subjects with type 1 diabetes for the assessment of closed-loop glucose controllers," *IEEE Transactions on Biomedical Engineering*, vol. 60, no. 12, pp. 3524–3533, 2013.

[9] C. Cobelli, C. Dalla Man, G. Sparacino, L. Magni, G. De Nicolao, and B. P. Kovatchev, "Diabetes: Models, signals, and control," *IEEE Reviews in Biomedical Engineering*, vol. 2, pp. 54–96, 2009.

[10] S. Schmidt, D. Boiroux, A. Ranjan, J. B. Jørgensen, H. Madsen, and K. Nørgaard, "An artificial pancreas for automated blood glucose control in patients with type 1 diabetes," *Therapeutic delivery*, vol. 6, no. 5, pp. 609–619, 2015.

[11] A. Haidar, "The artificial pancreas: How closed-loop control is revolutionizing diabetes," *IEEE Control Systems Magazine*, vol. 36, no. 5, pp. 28–47, 2016.

[12] Z. Mahmoudi, D. Boiroux, M. Hagdrup, N. Kj, H. Madsen, J. Bagterp, *et al.*, "Application of the continuous-discrete extended Kalman filter for fault detection in continuous glucose monitors for type 1 diabetes," in *2016 European Control Conference (ECC 2016)*, 2016, pp. 714–719.

[13] K. Turksoy, S. Samadi, J. Feng, E. Littlejohn, L. Quinn, and A. Cinar, "Meal detection in patients with type 1 diabetes: a new module for the multivariable adaptive artificial pancreas control system," *IEEE Journal of Biomedical and Health Informatics*, vol. 20, no. 1, pp. 47–54, 2016.

[14] J. Xie and Q. Wang, "A variable state dimension approach to meal detection and meal size estimation: in silico evaluation through basal-bolus insulin therapy for type 1 diabetes," *IEEE Transactions on Biomedical Engineering*, 2017.

[15] Z. Mahmoudi, K. Nørgaard, N. K. Poulsen, H. Madsen, and J. B. Jørgensen, "Fault and meal detection by redundant continuous glucose monitors and the unscented Kalman filter," *Biomedical Signal Processing and Control*, vol. 38, pp. 86–99, 2017.

[16] G. Marchetti, M. Barolo, L. Jovanovič, H. Zisser, and D. E. Seborg, "A feedforward-feedback glucose control strategy for type 1 diabetes mellitus," *Journal of Process Control*, vol. 18, no. 2, pp. 149–162, 2008.

[17] S. Schmidt, M. Meldgaard, N. Serifovski, C. Storm, T. M. Christensen, B. Gade-Rasmussen, and K. Nørgaard, "Use of an automated bolus calculator in MDI-treated type 1 diabetes," *Diabetes Care*, vol. 35, no. 5, pp. 984–990, 2012.

[18] D. Boiroux, T. Aradóttir, M. Hagdrup, N. Poulsen, H. Madsen, and J. B. Jørgensen, "A bolus calculator based on continuous-discrete unscented Kalman filtering for type 1 diabetics," in *9th IFAC Symposium on Biological and Medical Systems*, 2015, pp. 159 – 164.

[19] D. Boiroux, T. B. Aradóttir, K. Nørgaard, N. K. Poulsen, H. Madsen, and J. B. Jørgensen, "An adaptive nonlinear basal-bolus calculator for patients with type 1 diabetes," *Journal of Diabetes Science and Technology*, vol. 11, no. 1, pp. 29–36, 2017.

[20] R. Hovorka, J. M. Allen, D. Elleri, L. J. Chassin, J. Harris, D. Xing, C. Kollman, T. Hovorka, A. M. F. Larsen, M. Nodale, A. De Palma, M. E. Wilinska, C. L. Acerini, and D. B. Dunger, "Manual closed-loop insulin delivery in children and adolescents with type 1 diabetes: a phase 2 randomised crossover trial," *The Lancet*, vol. 375, pp. 743 – 751, 2010.

[21] R. Gondhalekar, E. Dassau, and F. J. Doyle, "Periodic zone-MPC with asymmetric costs for outpatient-ready safety of an artificial pancreas to treat type 1 diabetes," *Automatica*, vol. 71, pp. 237–246, 2016.

[22] D. Boiroux, A. K. Duun-Henriksen, S. Schmidt, K. Nørgaard, S. Madsbad, N. K. Poulsen, H. Madsen, and J. B. Jørgensen, "Overnight glucose control in people with type 1 diabetes," *Biomedical Signal Processing and Control*, vol. 39, pp. 503–512, 2018.

[23] K. Turksoy, E. S. Bayrak, L. Quinn, E. Littlejohn, and A. Cinar, "Multivariable adaptive closed-loop control of an artificial pancreas without meal and activity announcement," *Diabetes Technology & Therapeutics*, vol. 15, no. 5, pp. 386–400, 2013.

[24] C. Toffanin, R. Visentin, M. Messori, F. Di Palma, L. Magni, and C. Cobelli, "Towards a run-to-run adaptive artificial pancreas: In silico results," *IEEE Transactions on Biomedical Engineering*, vol. 99, p. DOI: 10.1109/TBME.2017.2652062, 2017.

[25] S. S. Kanderian, S. Weinzimer, G. Voskanyan, and G. M. Steil, "Identification of intraday metabolic profiles during closed-loop glucose control in individuals with type 1 diabetes," *Journal of Diabetes Science and Technology*, vol. 3, no. 5, pp. 1047 – 1057, 2009.

[26] A. Facchinetti, S. Del Favero, G. Sparacino, J. R. Castle, W. K. Ward, and C. Cobelli, "Modeling the glucose sensor error," *IEEE Transactions on Biomedical Engineering*, vol. 61, no. 3, pp. 620–629, 2014.

[27] R. Hovorka, V. Canonico, L. J. Chassin, U. Haueter, M. Massi-Benedetti, M. O. Federici, T. R. Pieber, H. C. Schaller, L. Schaupp, T. Vering, and M. E. Wilinska, "Nonlinear model predictive control of glucose concentration in subjects with type 1 diabetes," *Physiological Measurement*, vol. 25, pp. 905–920, 2004.

[28] G. Pillonetto, G. Sparacino, and C. Cobelli, "Numerical non-identifiability regions of the minimal model of glucose kinetics: superiority of bayesian estimation," *Mathematical Biosciences*, vol. 184, pp. 53 – 67, 2003.

[29] A. H. Jazwinski, *Stochastic Processes and Filtering Theory*. San Diego, CA: Academic Press, 1970.

[30] M. Nørgaard, N. K. Poulsen, and O. Ravn, "New developments in state estimation for nonlinear systems," *Automatica*, vol. 36, pp. 1627–1638, 2000.

[31] R. Schneider and C. Georgakis, "How to not make the extended kalman filter fail," *Industrial & Engineering Chemistry Research*, vol. 52, no. 9, pp. 3354–3362, 2013.

[32] J. B. Jørgensen and S. B. Jørgensen, "Comparison of prediction-error modelling criteria," in *Proceedings of the 2007 American Control Conference (ACC 2007)*, 2007, pp. 140–146.

[33] H. Singer, "Parameter estimation of nonlinear stochastic differential equations: simulated maximum likelihood versus extended Kalman filter and Itô-Taylor expansion," *Journal of Computational and Graphical Statistics*, vol. 11, no. 4, pp. 972–995, 2002.

[34] H. Madsen, *Time series analysis*. Chapman & Hall/CRC, 2007.

[35] C. Bohn and H. Unbehauen, "Sensitivity models for nonlinear filters with application to recursive parameter estimation for nonlinear state-space models," in *IEE Proceedings-Control Theory and Applications*, vol. 148, no. 2, 2001, pp. 137–145.

[36] J. B. Jørgensen, P. G. Thomsen, H. Madsen, and M. R. Kristensen, "A computationally efficient and robust implementation of the continuous-discrete extended Kalman filter," in *American Control Conference 2007 (ACC'07).*, 2007, pp. 3706–3712.

[37] D. Boiroux, R. Juhl, H. Madsen, and J. B. Jørgensen, "An efficient UD-based algorithm for the computation of maximum likelihood sensitivity of continuous-discrete systems," in *55th Conference on Decision and Control (CDC)*. IEEE, 2016, pp. 3048–3053.

[38] R. Hovorka, F. Shojaee-Moradie, P. V. Caroll, L. J. Chassin, I. J. Gowrie, N. C. Jackson, R. S. Tudor, A. M. Umpleby, and R. H. Jones, "Partitioning glucose distribution/transport, disposal, and endogenous production during IVGTT," *American Journal of Physiology*, vol. 282, pp. 992–1007, 2002.

[39] M. E. Wilinska, L. J. Chassin, C. L. Acerini, J. M. Allen, D. B. Dunger, and R. Hovorka, "Simulation environment to evaluate closed-loop insulin delivery systems in type 1 diabetes," *Journal of Diabetes Science and Technology*, vol. 4, no. 1, pp. 132 – 144, 2010.

[40] G. Maruyama, "Continuous Markov processes and stochastic equations," *Rendiconti del Circolo Matematico di Palermo*, vol. 4, no. 1, pp. 48–90, 1955.

[41] K. J. Åström, "Maximum likelihood and prediction error methods," *Automatica*, vol. 16, no. 5, pp. 551–574, 1980.